SCIENTIFIC REPORTS

OPEN

Observation of an atomic exchange bias effect in DyCo$_4$ film

Kai Chen[1], Dieter Lott[2], Florin Radu[3], Fadi Choueikani[1], Edwige Otero[1] & Philippe Ohresser[1]

The fundamental important and technologically widely employed exchange bias effect occurs in general in bilayers of magnetic thin films consisting of antiferromagnetic and ferromagnetic layers where the hard magnetization behavior of an antiferromagnetic thin film causes a shift in the magnetization curve of a soft ferromagnetic film. The minimization of the single magnetic grain size to increase the storage density and the subsequent demand for magnetic materials with very high magnetic anisotropy requires a system with high H_{EB}. Here we report an extremely high H_{EB} of 4 Tesla observed in a single amorphous DyCo$_4$ film close to room temperature. The origin of the exchange bias can be associated with the variation of the magnetic behavior from the surface towards the bulk part of the film revealed by X-ray absorption spectroscopy and X-ray magnetic circular dichroism techniques utilizing the bulk sensitive transmission and the surface sensitive total electron yield modes. The competition between the atomic exchange coupling in the single film and the Zeeman interaction lead to an intrinsic exchanged coupled system and the so far highest exchange bias effect $H_{EB} = 4$ Tesla reported in a single film, which is accommodated by a partial domain wall formation.

Exchange bias effect (EB) was discovered in 1956 by Meiklejohn and Bean when studying Co particles embedded in their native antiferromagnetic oxide[1]. It is generally considered to form from an uncompensated spin configuration at the ferromagnetic/antiferromagnetic (FM/AF) interface[2,3], as it is the case in small particles, inhomogeneous materials, FM films on AF single crystals and FM on AF thin films[4] with frozen and rotatable spins at their interfaces[5–9]. Phenomenologically, the EB effect in FM/AF systems displays a shift of the hysteresis by an EB field H_{EB} that is achieved by a magnetic field cooling procedure down to the Néel temperature T_N of the AF. The experimentally observed value of the H_{EB} in FM/AF systems, however, is in general several orders of magnitude below the theoretical prediction for a perfect EB system[10]. This discrepancy resulted in a heavy debate and the development of sophisticated models for the explanation of the origin of the EB effect and its drastic reduction of the EB effect in real EB systems[4,11,12]. Besides the classical system of AF/FM interfaces, EB and related effects have been observed also in other types of samples, e.g. involving ferrimagnets (FI): AF/FI[13], FI/FM[14–16] and lately also in FI/FI[17] with a compensated spin structures at the interface. Transition Metal-Rare Earth (TM-RE) alloys, in particular, are nowadays suggested to used as FI materials in magnetic hybrid structures exhibiting strong EB effects[18].

Besides an interfacial exchange between two chemically and magnetically different compositions, a physically induced magnetic phase deviation from the bulk to the surface may also results into an exchange bias effect although there is no obvious chemical interface in the sample. The lower atomic coordination of the atoms at the surface results in a band narrowing, leading to changes of the moments at the surface in respect to the bulk. In MnF$_2$ [19,20], it requires a lower magnetic field value to force the phase transition from an AF to a spin-flop state at the surface. Ferromagnetism on the surface of the bulk paramagnetic intermetallic compound YCo$_2$ was predicted using full-potential electronic structure calculations[21] and observed by spin-resolved photoelectron spectroscopy[22]. For rare earth materials, surface enhanced magnetic ordering have been found in Gd[23] and Tb[24] resulting in an increase of the Curie temperature for the surface states. Following the theoretical calculations performed by Camley *et al.*[25], the surface phase transitions are responsible for the twisted magnetic spin structures observed in Fe/Gd multilayer[26–30].

Figure 1 shows a schematic sketch of a single ferrimagnetic film system with the potential of intrinsic exchange bias effect. Surface and bulk of the film are of the same composition consisting here of two magnetic sites that are strongly exchanged coupled to each other but possess opposite signs in their resulting moments. If the surface and bulk parts are again exchanged coupled to each other, their different magnetic behavior in respect to an external

[1]Synchrotron SOLEIL, L'Orme des Merisiers, Saint-Aubin-BP48, 91192 GIF-sur-YVETTE CEDEX, France. [2]Institute for Materials Research, Helmholtz-Zentrum Geesthacht, 21502 Geesthacht, Germany. [3]Helmholtz-Zentrum Berlin für Materialien und Energie, Albert-Einstein-Str.15, 12489 Berlin, Germany. Correspondence and requests for materials should be addressed to K.C. (email: kaichen.hzg@gmail.com)
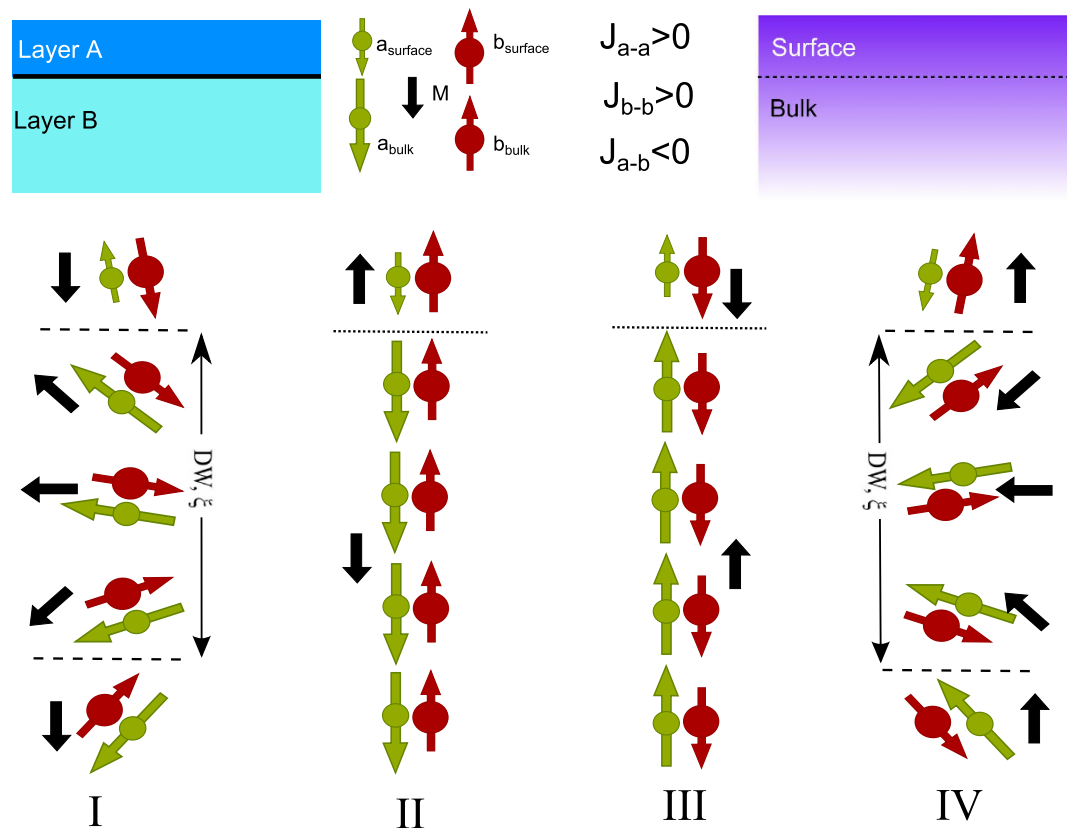
Figure 1. Sketch of the exchange bias system from single layer with different surface and bulk magnetism. The classical bilayer model is also shown for a better understanding. Both the layer A and B are ferrimagnetic materials consisting of antiparallel coupled atoms of Dy and Co. The layers A (or surface) and B (or bulk) are dominated by Dy and Co, respectively. There exist four different magnetic phases marked as I, II, III and IV with different magnetic field, with out of plane domain wall formed in I and IV.

applied magnetic field may lead to an competition between the Zeeman and the exchange coupling energy that potentially creates an EB system without the necessity of an additional magnetic layer. When no magnetic field is applied, the magnetization behavior of the surface layer follows the one of the bulk due to the exchange coupling, marked as II and III. When an sufficient high external magnetic field is applied, the Zeeman energy term will dominate for the surface layer and turn its resulting moment along the applied magnetic field direction. Thus state I or IV forms with an out-of-plane domain wall (DW) of a length of ξ. With respect to a classical EB system, there is no chemical interface in the EB system and therefore the EB effect is expected to be mediated by the formation of a domain wall. Since there is no contamination, pinhole effect and interfacial roughness that may reduce the EB strength, such a system has the potential to show large EB values.

In this paper we report the largest so far observed EB value measured in a single amorphous RE-TM alloy consisting of Dy and Co with a chemical composition of $DyCo_4$. In this strongly atomically exchanged coupled system the surface and the rest of the film exhibit clear differences in their magnetic behavior with magnetic field and temperature. At a temperature of $T = 270\,K$, the exchange coupling between the surface and the bulk states leads to the emergence of an additional asymmetric magnetic hysteresis loop with its center shifted by about $\mu_0 H_{EB} = 4\,T$. Such a giant EB is observed for the first time originating from the atomic exchange coupling between a virtual surface part and the bulk part in $DyCo_4$ without a chemical interface. This may be useful for creating novel magnetic exchange bias systems for future magnetic storage application by compacting several layers of a spin-valve system into a single one.

Samples and Experimental set-up

The $DyCo_4$ samples were prepared by magnetron sputtering (MAGSSY chamber at BESSY) in an ultraclean argon atmosphere of 1.5×10^{-3} mbar with a base pressure of $p < 5 \times 10^{-9}$ mbar at the deposition temperature of $300\,K$. The stoichiometry of the ferrimagnetic alloys was controlled by setting the deposition rate of separate chemical elements in a co-evaporation scheme. Si_3N_4 membranes with a surface area of $5 \times 5\,mm^2$ and a thickness of $100\,nm$ were used as substrates for the soft x-ray transmission measurements. A capping layer of $3\,nm$ of tantalum(Ta) was grown on the $50\,nm$ thick $DyCo_4$ layer to prevent surface oxidation. As a capping layer to prevent oxidation, Ta layer have been used and commonly considered to have no influence to the macroscopic magnetism of the layer underneath[17,31]. However, In our case we observe a rather large difference between the surface and the bulk XMCD spectra. We believe that this large difference is caused mainly by noncollinearity (conical-like) in the magnetic structure of $DyCo_4$. Also, considering the ferrimagnetism of $DyCo_4$, the surface atoms have different
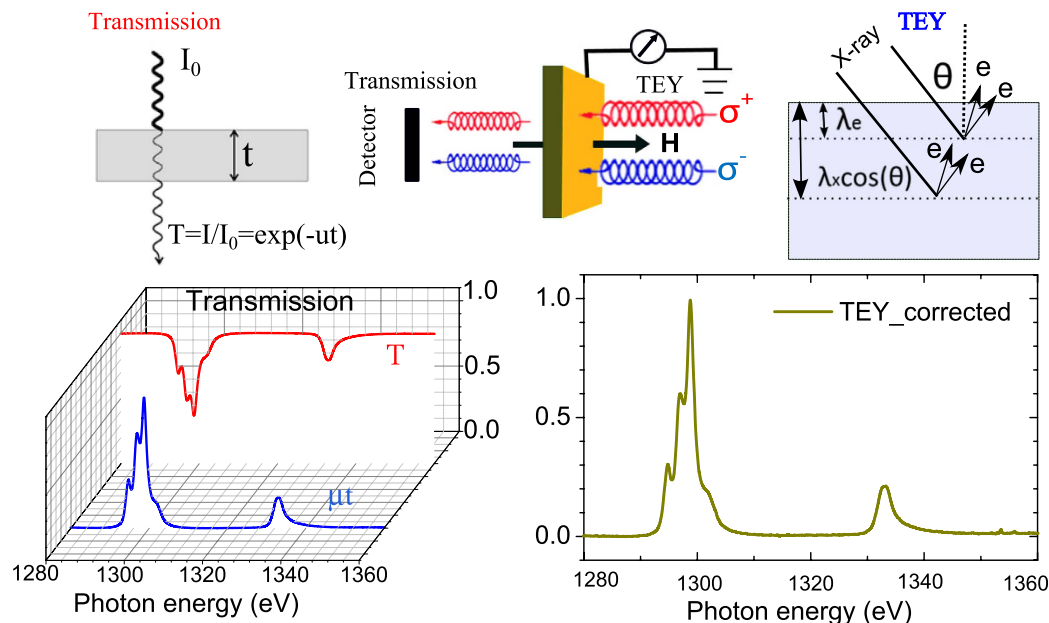
Figure 2. Experimental setup for surface and bulk magnetism. (Up)XMCD measurements of transmission and TEY mode, the transmitted x-ray intensities and total electron yield from the sample are recorded. (Down) The XAS was extracted as the logarithm of the ratio of the transmitted x-ray intensities, or the drain current from the sample after the correction of the saturation effect.

chemical environments and the exchange coupling energy between Dy and Co may be smaller due to the reduced coordination number. As a result, these two effects may concur contributing to the observed differences between the bulk and the surface magnetism.

X-ray absorption and XMCD spectra at the Co $L_{2,3}$ and Dy $M_{4,5}$ edges were measured at temperatures from 4.4 K to 300 K in transmission geometry at the synchrotron facility SOLEIL using the 7T cryomagnet installed on the DEIMOS (Dichroism Experimental Installation for Magneto-Optical Spectroscopy) beamline[32,33]. The XMCD studies were carried out using x-rays of circular right (CR) and left (CL) polarizations with a magnetic field of $\mu_0H = 6T$ applied along the x-ray beam (see Fig. 2). For the magnetic sensitivity to the individual magnetic elements, the characteristic energies for the Co $L_{2,3}$ and the Dy $M_{4,5}$ edges were selected. The XMCD data were recorded as $(\sigma^+ - \sigma^-)$, where σ^+ and σ^- denote the absorption cross section for CR and CL polarized x-rays, respectively. The magnetic hysteresis measurements were performed by taking the difference of $(\sigma^+ - \sigma^-)$ with the photon energy for the x-ray beam set to the value at the L_3 edge of Co or M_5 edge of Dy where the XMCD signal is maximized. For the transmission measurements[34], the experimental XMCD is extracted as the logarithm of the ratio of the transmitted x-ray intensities of different polarization states and probes the whole sample. The total electron yield (TEY) signal was recorded at the same time giving a high surface sensitivity with a sampling depths λ_e of ~2 nm[35,36]. As long as the sampling depth remains much shorter than the x-ray attenuation length $\lambda_x\cos(\theta)$ (with $\theta = 0$ in our experiments), the TEY signal represents the true XAS and XMCD with the accuracy of ~5 − 10%[35,37] compared to the results after the correction of the saturation effects. The combination of both methods allows one to separate the surface from the bulk contributions.

Experimental results

In amorphous Dy_xCo_{100-x} the magnetic configuration is determined by the competition between the magnetic atomic exchange interaction and the Zeemann interaction. The latter favors the Co and the Dy magnetic moments being aligned both in the direction of the applied magnetic field, while the atomic exchange interaction is minimized if Dy and Co atoms are in an antiferromagnetic configuration. The strong exchange interaction in Dy_xCo_{100-x} between the sites forces them in general into an AF alignment while their resulting moment is turned into the direction of the applied magnetic field. One of the intriguing properties of amorphous systems consisting of two magnetic different sites belonging to the RE and TM series, respectively, is the different temperature dependence of their magnetic moment resulting into a change of the magnetically dominant site. In Dy_xCo_{100-x}, Dy possesses at low temperatures a much larger magnetic moment compared to the one of Co. On the other hand, the Dy moment decays much stronger with increasing temperature until the compensation temperature T_{comp} is reached when the total magnetic moment of both sites are equal. At temperatures higher than T_{comp} the compound enters into the Co dominant phase accompanied with a reversal of the orientation for both sites due to the strongly AF exchanged coupling between both magnetic sites. T_{comp} depends on the individual composition and can be controlled by the composition parameter x, and is expected to be ~250 K for $DyCo_4$.

X-ray absorption spectroscopy (XAS) and XMCD measurements were carried out at the Co $L_{2,3}$ and the Dy $M_{4,5}$ edges for a series of temperatures, utilizing the bulk sensitive transmission and the surface sensitive total electron yield (TEY) modes. The spectra for T = 4.4 K from transmission measurements taken at an applied
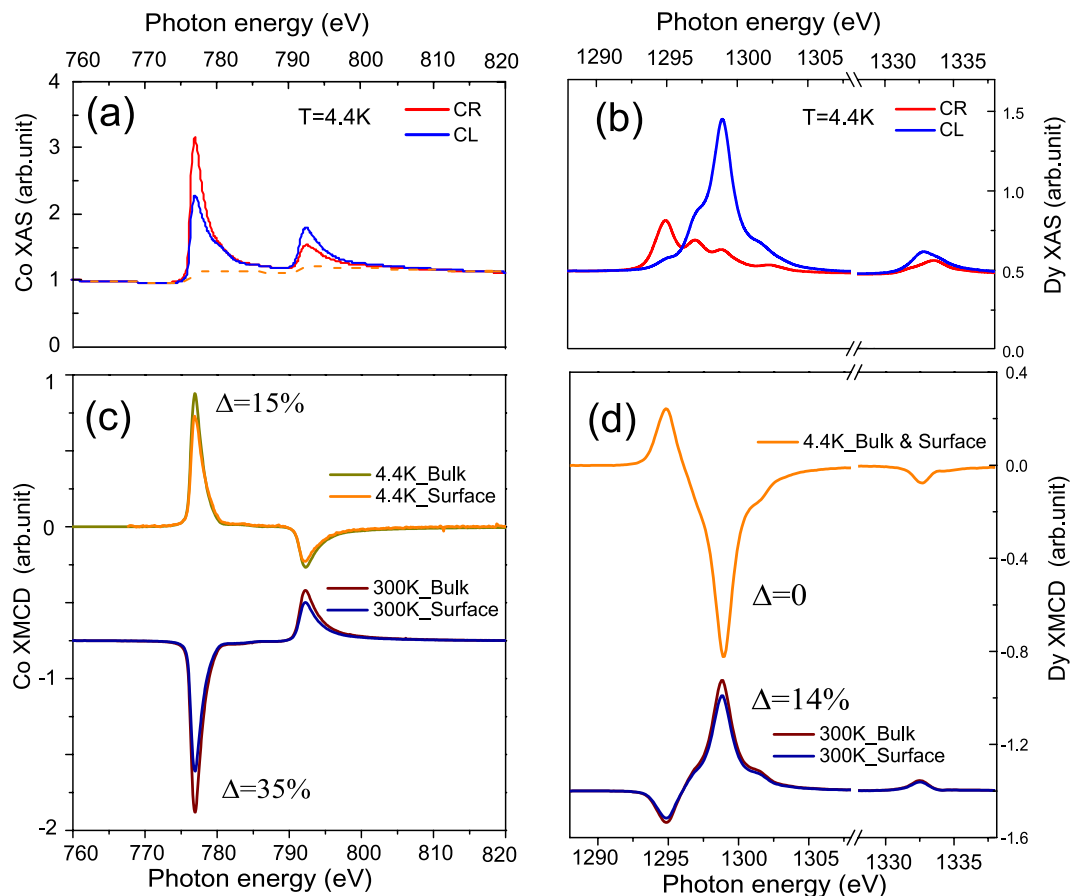
Figure 3. XAS and XMCD of Co and Dy. XAS at the Co $L_{2,3}$ (**a**) and Dy $M_{4,5}$ (**b**) with the magnetic field of $\mu_0H = 6T$ applied out of plane at $T = 4.4\,K$. Surface and bulk XMCD of Co (**c**) and Dy (**d**) at $T = 4.4\,K$ and 300 K. For Co, the surface XMCD signal is ~15% and 34% reduced compared to the bulk at 4.4 and 300 K, respectively. For Dy, the surface XMCD signal is the same or 14% reduced compared to the bulk at 4.4 or 300 K, respectively. A more reduced Co surface magnetism at high temperature is observed compared to that of Dy.

magnetic field of $\mu_0H = 6T$ are shown for the Co and Dy site in Fig. 3(a,b), respectively. The resulting surface and bulk XMCD spectra of Co and Dy at $\mu_0H = 6T$ are displayed in Fig. 3(c,d) for $T = 4.4\,K$ and 300 K. The positive (negative) XMCD signal of Co (Dy) at 4.4 K indicates here that the out of plane projection of the magnetic moment M_z^{Co} (M_z^{Dy}) is antiparallel (parallel) aligned along the applied magnetic field as expected for the Dy dominated magnetic state at low temperatures. At $T = 300\,K$ a clear change of the sign in the XMCD signal at both absorption edges is observed indicating that the out of plane projections of the magnetic moments M_z^{Co} and M_z^{Dy} have reversed their direction and $DyCo_4$ with a compensation temperature below is now in the Co dominated state. Interestingly, the bulk XMCD signal for Co is about 15% higher in magnitude at 300 K compared to that of 4.4 K, while for Dy the XMCD signal is about 45% reduced in magnitude for the higher temperature. The reduction of the moment at low temperature may be explained by the formation of a cone structure at low temperatures as it is observed in other rare earth materials as e.g. Ho[38] or in similar $RECo_5$ compounds[39]. At higher temperatures, the decrease of the XMCD signal for the Dy site indicates the decrease of the Dy moment with temperature. For both temperatures a clear deviation between the XMCD signal from the TEY and the transmission measurements is observed for the Co site. The surface sensitive XMCD signal at the Co edge from TEY is ~15% and 34% reduced compared to that bulk sensitive XMCD from transmission at $T = 4.4\,K$ and 300 K, respectively. For the Dy site the effect is much smaller. At 4.4 K, no significant differences can be observed, while at 300 K the surface moments is only 14% reduced compared to bulk. It should be noted that the TEY data is already corrected for the reduction of the signal due to saturation effects by ~$5 - 10\%$[35,37]. Since TEY probes only the first few nanometers (~2 nm) at the surface and the transmission measurement is sensitive to the magnetism of the complete film with a thickness of 50 nm with the surface magnetism giving only a tiny contribution of ~4%, it can be concluded that the magnetism at the surface (denoted as the surface part) differs significantly from the rest of the film (denoted here as the bulk part).

By the application of the sum rules[34,40,41] for the measured XAS and XMCD spectra, the bulk magnetic moments of Dy and Co are determined to $M_z^{Dy} = 7.60 \pm 0.70\mu_B/atom$ and $M_z^{Co} = -1.30 \pm 0.20\mu_B/atom$ at $T = 4.4\,K$, and $M_z^{Dy} = -4.00 \pm 0.40\mu_B/atom$ and $M_z^{Co} = 1.60 \pm 0.20\mu_B/atom$ at 300 K, respectively. The magnetic dipole term T_z associated with the spin-dependent asphericity of the electronic cloud can be neglected for Co[34], but not for the rare earth element Dy[41] where it can be approximated as $-\frac{2}{3}\langle S_z^{eff}\rangle$. One should note that the XMCD signals
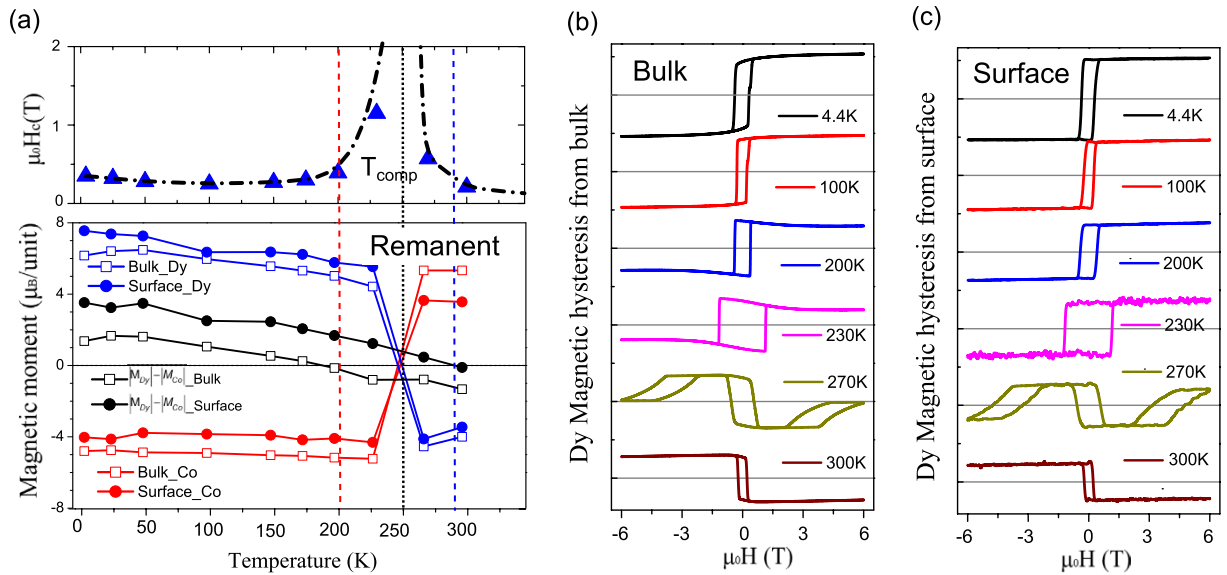
Figure 4. Temperature dependent magnetic properties of Dy and Co. (a) (up) Coercivity $\mu_0 H_c$ from the temperature dependent magnetic hysteresis loops and (down) the remanent bulk and surface magnetic moments of Dy and Co, respectively. The values of $|M_{Dy}| - |M_{Co}|$ of the bulk and surface are also listed showing significant differences. The error bar from the sum-rule calculations (~%10) are not shown, the statistic error bar (~%4) are smaller than the size of the points. Panels (**b,c**) show the temperature dependent (4.4–300 K) Dy magnetic hysteresis loops for the Dy site taken by XMCD measurements for the bulk and the surface parts, respectively.

$(\sigma^+ - \sigma^-)$ as well as the magnetic moments for Co and Dy have opposite signs at both temperatures, demonstrating their antiparallel alignment. At T = 4.4 K, the magnetic configuration is in the Dy dominant phase in which M_z^{Dy} is pointing along the direction of the applied magnetic field while at T = 300 K, the situation is reversed in the Co dominant phase with now M_z^{Co} aligning along the magnetic field direction. At low temperatures as T = 4.4 K Dy possesses a magnetic moment as high as 10 μ_B/atom with J = 15/2. The significantly lower value found here in the alloy indicates that the magnetic moments of Dy are not completely aligned along the applied magnetic field direction since the XMCD method is only sensitive to the moments projection along the magnetic field direction. This may be explained by the formation of a cone spin structure of Dy as already mentioned before and account also for the reduction of M_z^{Co} at low temperatures due to the strong antiferromagnetic coupling between Co and Dy. Temperature dependent magnetic hysteresis loops were recorded at the photon energies where the XMCD signals for both elements Dy (E = 1298.4 eV) and Co (E = 778 eV) were largest. Figure 4 shows the temperature dependent hysteresis loops recorded at the Dy absorption edges in the bulk sensitive transmission (Fig. 4(b)) and in surface sensitive TEY mode (Fig. 4(c)). The hysteresis loops taken at the Co absorption edge (see SI) follow the Dy hysteresis loops demonstrating the antiparallel exchange coupling between both elements in the alloy for all temperatures. To determine the compensation temperature at which the total magnetic contributions from Dy and Co are equal, i.e. when the net magnetic moment of the alloy becomes zero, the coercivity $\mu_0 H_c$ is plotted as a function of temperature shown in Fig. 4(a). The steep increase and decrease of the value of the coercivity $\mu_0 H_c$ at 230 K and 270 K, respectively, can be fitted by exponential functions. By the determination of their common asymptote, T_{comp} can be estimated to about 250 K. The lower panel of Fig. 4(a) shows the bulk and surface magnetic moments of Dy and Co, respectively, for various temperatures from 4.4 K to 300 K at remanence calculated by the sum rules. For both parts, the total moments for Dy and Co undergo a change of their magnetization direction in respect to the applied magnetic field at around 250 K as it is expected at T_{comp}. The resulting magnetic moments, calculated by taking the difference of the total magnetization for both sites, $|M_{Dy}| - |M_{Co}|$, however, show significantly deviations from the overall determined T_{comp}. The resulting moment for the bulk part already reverses its sign at ~200 K, while the surface part remains in the Dy dominant phase up to ~290 K demonstrating a clear magnetic phase separation between the surface and the bulk state of the film in this temperature regime.

By using the transmission and TEY mode, the temperature dependent magnetization behavior is surveyed for the bulk and surface state of the film separately as it is shown in Fig. 4(b,c), respectively. For both series of hysteresis loops the temperature dependent transition from the dominate Dy to the dominate Co magnetic state is observed, however, the saturation behavior shows clear differences in the bulk and surface part, particularly around the compensation temperature. The bulk magnetization M_z^{bulk} exhibits at T = 200 K a clear reduction at higher magnetic fields that becomes even more pronounced by approaching the compensation temperature. The surface part, on the other hand, displays a square shape of the hysteresis loops that remain unchanged even close to the transition temperature. Such differences in the behavior of bulk and surface magnetization indicates the formation of a domain wall with a partial winding that takes place deeper in the sample.

Particularly interesting is the magnetic behavior at a temperature slightly higher than the compensation temperature, when the film is supposed to enter into the Co dominated magnetic state. As expected for a change from the Dy to Co

5
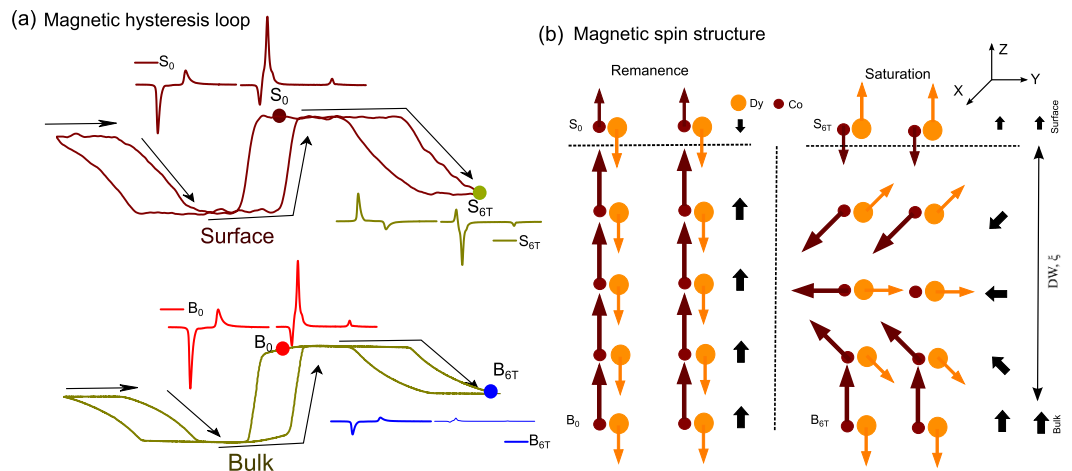
Figure 5. Magnetic spin configuration at T = 270 K. (**a**) Surface and bulk magnetic hysteresis loops of Dy at 270 K. XMCD of Dy and Co at the 4 states of S_0, S_{6T}, B_0 and B_{6T} marked in the hysteresis are also shown. With $\mu_0 H = 6T$, opposite magnetization from the surface to the bulk is observed. (**b**) Sketch of the spin structure of $DyCo_4$ at 270 K for the remanant and saturation state with an out of plane magnetic domain wall from the surface to the bulk.

dominant state, the remanent magnetization flips its sign at T = 270 K compared to the situation below T_{comp}. On the other hand, additional "wing shape" hysteresis loops can be observed when $6T > \mu_0 H > 2T$ and $-6T < \mu_0 H < -2T$. At $\mu_0 H = 6T$, M_z^{bulk} is almost zero while $M_z^{surface}$ reverses its magnetization direction to a non-zero value. Cycling the magnetic field between $6T > \mu_0 H > 0T$ or $-6T < \mu_0 H < 0T$, results into an asymmetric hysteresis loop with two magnetically distinct states. Considering the definition of the exchange bias field H_{EB} as a shift of the center of the hysteresis loop from zero field, we observe here a extremely high H_{EB} of around 4T. The cycling between these high and zero fields show that the shape of the loops and H_{EB} remains constant without observable training effects.

Discussion

In order to understand the peculiar behavior at T = 270 K with its addition wing shape hysteresis loops at higher magnetic fields, the individual magnetic behavior of the surface and the bulk part as well as their interplay have to be considered. For low magnetic fields, when the Zeeman interaction is weak and the exchange interaction is the dominating term, it is energetically favorable for the system that the Dy dominant surface part follows the bulk magnetism that is already in the Co dominant state. The system remains magnetically stable up to approximately $\mu_0 H = 4T$, when the Zeeman interaction becomes finally strong enough to compete with the exchange interaction of the system resulting into a rotation of the magnetically strongly coupled Dy and Co in the surface part with M_z^{Dy} aligning along the applied magnetic field direction. For the bulk configuration, on the other hand, the reversal of the surface magnetization leads to a domain wall configuration to store the exchange energy which is release back when the Zeeman energy is reduced again analogue to the situation just below T_{comp}. This is reflected in the reduction of the magnetization projection M_z^{bulk} for Dy and Co driven by the surface magnetization as indicated by the correlated hysteresis loops between surface and bulk parts. Figure 5(b) shows schematically the magnetic configurations in the film for the two distinct states in the wing hysteresis. In the lower magnetic state, the resulting moment is determined by $M_z^{bulk} = (M_z^{Co,bulk} - M_z^{Dy,bulk}) > 0$ while $M_z^{surface} = (M_z^{Co,surface} - M_z^{Dy,surface}) < 0$. At this state, $M_z^{surface}$ aligns antiparallel to the magnetic field due to the exchange coupling with the bulk part, as the identical signs in the XMCD signals in Fig. 5(a) reveal.

In the higher magnetic state resulting $M_z^{surface}$ aligns now parallel along the field direction while M_z^{bulk} is reduced due to the formation of a complex domain winding state. The occurrence of the wing shape hysteresis loops shows that the surface and bulk states of the film are strongly magnetically coupled by the atomic exchange interaction keeping the two magnetic states stable in a certain magnetic field range. At high fields, from the interface to the bulk, an out of plane domain wall is formed with the wall energy σ_w stored in the boundary. According to the Mauri's model[11], the atomic exchange field can be described as: $H_{EB} = A/(\xi \cdot M_{surface})$, where A is the atomic exchange stiffness, ξ is the thickness of the domain wall as shown in Fig. 5(b) and $M_{surface}$ is the surface magnetization. At low magnetic fields the magnetically softer bulk part determines the magnetism of the system while at higher magnetic fields the magnetically harder surface layer becomes the trigger of the change in the magnetic configuration. Since here the atomic exchange between both sides is crucial for the observed phenomena of the huge shift of the wing shape hysteresis loop, this effect is named atomic exchange bias effect.

It is reasonable that an out-of-plane magnetic domain wall expands throughout the film of 50 nm. According to Mauris model, the domain wall width can by estimated according to the following relationship: $\xi = \pi \sqrt{A/K}$, with A and K being the exchange stiffness and exchange anisotropy. Assuming the parameter A and K for $DyCo_4$ to be similar to that of TbFe at 300 K[42], which are $A = 8 * 10^{-8}$ erg/cm and $K = 2.8 * 10^4$ erg/cm³, the resulting domain wall equals to ~53 nm.

In conclusion, a huge exchange bias effect with H_{EB} was observed in a single $DyCo_4$ alloy film by using synchrotron soft x-ray magnetic circular spectroscopies at the Dy $M_{4,5}$ and Co $L_{2,3}$ edges in transmission and TEY mode.

It was found that the magnetism on the surface behaves drastically different as in the bulk of the $DyCo_4$ film. At $T = 270$ K just above the T_{comp}, the bulk magnetism is dominated by the Co cite while the surface magnetism is still in the Dy dominant state due to the strong reduction of the Co magnetization at the surface. The strong atomic exchange interaction couples the surface and bulk part leading to two magnetic stable states that can be observed as wing shape hysteresis loops at high magnetic fields, which also exhibits an asymmetric behavior. Such a giant exchange bias effect of up to $\mu_0 H_{EB} = 4T$ is reported for the first time for a single film without an additional chemical interface. The availability of large exchange bias effects may be of great importance for future magnetic data storage devices for making use of materials with extremely high magnetic anisotropy.

References

1. Meiklejohn, W. H. & Bean, C. P. New magnetic anisotropy. *Phys. Rev.* **102,** 1413 (1956).
2. Kappenberger, P. *et al.* Direct imaging and determination of the uncompensated spin density in exchange-biased CoO/(CoPt) multilayers. *Phys. Rev. Lett.* **91,** 267202 (2003).
3. Valev, V. K., Gruyters, M., Kirilyuk, A. & Rasing, Th. Direct observation of exchange bias related uncompensated spins at the CoO/Cu interface. *Phys. Rev. Lett.* **96,** 067206 (2006).
4. Nogués, J. & Shuller, Ivan. K. Exchange bias. *J. Magn. Magn. Mater.* **192,** 203 (1999).
5. Ohldag, H. *et al.* Correlation between exchange bias and pinned interfacial spins. *Phys. Rev. Lett.* **91,** 017203 (2003).
6. Radu, F. *et al.* Origin of the reduced exchange bias in an epitaxial FeNi(111)/CoO(111) bilayer. *Phys. Rev. B* **79,** 184425 (2009).
7. Mishra, S. K. *et al.* Dual behavior of antiferromagnetic uncompensated spins in NiFe/IrMn exchange biased bilayers. *Phys. Rev. B* **81,** 212404 (2010).
8. Wu, J. *et al.* Direct measurement of rotatable and frozen CoO spins in exchange bias system of CoO/Fe/Ag(001). *Phys. Rev. Lett.* **104,** 217204 (2010).
9. Ge, C. *et al.* Direct observation of rotatable uncompensated spins in the exchange bias system Co/CoOMgO. *Nanoscale* **5,** 10236–10241(2013).
10. Radu, F. & Zabel, H. Magnetic heterostructures. *Springer Tracts Mod. Phys.* **227,** 97184 (2008).
11. Mauri, D., Siegmann, H. C., Bagus, P. S. & Kay, E. Simple model for thin ferromagnetic films exchange coupled to an antiferromagnetic substrate. *J. Appl. Phys.* **62,** 3047 (1987).
12. Jungblut, R., Coehoorn, R., Johnson, M. T., Stegge, J. aan de & Reinders, A. Orientational dependence of the exchange biasing in molecular-beam-epitaxy-grown $Ni_{80}Fe_{20}/Fe_{50}Mn_{50}$ bilayers. *J. Appl. Phys.* **75,** 6659 (1994).
13. Van der Zaag, P. J. *et al.* A study of the magnitude of exchange biasing in [111] Fe_3O_4/CoO bilayers. *J. Magn. Magn. Mater.* **148,** 346 (1995).
14. Hellman, F., van Dover, R. B. & Gyorgy, E. M. Unexpected unidirectional anisotropy in amorphous Tb-Fe/Ni-Fe-Mo bilayer films. *Appl. Phys. Lett.* **50,** 296 (1987).
15. Cain, W. C. & Kryder, M. H. Investigation of the exchange mechanism in NiFe-TbCo bilayers. *J. Appl. Phys.* **67,** 5722 (1990).
16. Schubert, C. *et al.* Interfacial exchange coupling in Fe-Tb-/[Co/Pt] heterostructures. *Phys. Rev. B* **87,** 054415 (2013).
17. Radu, F., Abrudan, R., Radu, I., Schmitz, D. & Zabel, H. Perpendicular exchange bias in ferrimagnetic spin valves. *Nat. Commun.* **3,** 715 (2012).
18. Radu, F. inventors; Spin-Valve, United States patent US 14,383,131. 2015 Mar 12.
19. Mills, D. L. Surface spin-flop state in a simple antiferromagnet. *Phys. Rev. Lett.* **20,** 18 (1968).
20. Keefer, F. & Chow, H. Dynamics of the antiferromagnetic spin-flop transition. *Phys. Rev. Lett.* **31,** 1061 (1973).
21. Khmelevskyi, S., Mohn, P., Redinger, J. & Weinert, M. Magnetism on the surface of the bulk paramagnetic intermetallic compound. *Phys. Rev. Lett.* **94,** 146403 (2005).
22. Dedkov, Yu. S. *et al.* Yco_2: intrinsic magnetic surface of a paramagnetic bulk material. *Phys. Rev. Lett.* **99,** 047204 (2007).
23. Weller, D., Alvarado, S. F., Gudat, W., Schröder, K. & Campagna, M. Observation of surface-enhanced magnetic order and magnetic surface reconstruction on Gd(0001). *Phys. Rev. Lett.* **54,** 1555 (1985).
24. Rau, C., Jin, C. & Robert, M. Ferromagnetic order at Tb surfaces above the bulk Curie temperature. *J. Appl. Phys.* **63,** 3667 (1988).
25. LePage, J. G. & Camley, R. E. Surface phase transitions and spin-wave modes in semi-infinite magnetic superlattices with antiferromagnetic interfacial coupling. *Phys. Rev. Lett.* **65,** 1152 (1990).
26. McGrath, O. F. K. *et al.* Observation and interpretation of a partial Gd twisted spin state in an epitaxial Gd/Fe bilayer. *Phys. Rev. B* **54,** 6088 (1996).
27. Kravtsov, E., Haskel, D., te Velthuis, S. G. E., Jiang, J. S. & Kirby, B. J. Complementary polarized neutron and resonant x-ray magnetic reflectometry measurements in Fe/Gd heterostructures: Case of inhomogeneous intralayer magnetic structure. *Phys. Rev. B* **79,** 134438 (2009).
28. Haskel, D. *et al.* Enhanced Interfacial Magnetic Coupling of Gd/Fe Multilayer. *Phys. Rev. Lett.* **87,** 207201 (2001).
29. Koizumi, A., Takagaki, M., Suzuki, M., Kawamura, N. & Sakai, N. Anomalous magnetic hysteresis of Gd and Fe moments in a Gd/Fe multilayer measured by hard x-ray magnetic circular dichroism. *Phys. Rev. B* **61,** R14909 (2000).
30. Haskel, D. *et al.* Nature of inhomogeneous magnetic state in artificial Fe/Gd ferrimagnetic multilayers. *Phys. Rev. B* **67,** R180406 (2003).
31. Tang, M. H., Zhang, Z., Tian, S. Y., Wang, J., Ma, B. & Jin, Q. Y. Interfacial exchange coupling and magnetization reversal in perpendicular $[Co/Ni]_N$/TbCo composite structures. *Sci. Rep* **5,** 10863 (2015).
32. Ohresser, P. *et al.* DEIMOS: a beamline dedicated to dichroism measurements in the 350-2500 eV energy range. *Rev. Sci. Instrum.* **85,** 013106 (2014).
33. Chen, K. *et al.* Temperature-dependent magnetic properties of ferrimagnetic $DyCo_3$ alloy films. *Phys. Rev. B* **91,** 024409 (2015).
34. Chen, C. T. *et al.* Experimental confirmation of the x-ray magnetic circular dichroism sum rules for Iron and Cobalt. *Phys. Rev. Lett.* **75,** 152 (1995).
35. Nakajima, R., Stöhr, J. & Idzerda, Y. U. Electron-yield saturation effects in L-edge x-ray magnetic circular dichroism spectra of Fe, Co, and Ni. *Phys. Rev. B* **59,** 6421 (1999).
36. Lee, J. *et al.* A direct test of x-ray magnetic circular dichroism sum rules for strained Ni films using polarized neutron reflection. *J. Phys. Condens. Matter* **9,** L137 (1997).
37. O'Brien, W. L. & Tonner, B. P. Orbital and spin sum rules in x-ray magnetic circular dichroism. *Phys. Rev. B* **50,** 12672 (1994).
38. Koehler, W. C., Cable, J. W., Wilkinson, M. K. & Wollan, E. O. Magnetic Structures of Holmium. I. The Virgin State. *Phys. Rev.* **151,** 414 (1966).
39. Zhao, T., Jin, H., Guo, G., Han, X. & Chen, H. Magnetic properties of R ions in RCo5 compounds (R=Pr, Nd, Sm, Gd, Tb, Dy, Ho, and Er). *Phys. Rev. B* **43,** 8593 (1991).
40. Thole, B. T., Carra, P., Sette, F. & van der Laan, G. X-ray circular dichroism as a probe of orbital magnetization. *Phys. Rev. Lett.* **68,** 1943 (1992).
41. Carra, P., Thole, B. T., Altarelli, M. & Wang, X. X-ray circular dichroism and local magnetic fields. *Phys. Rev. Lett.* **70,** 694 (1993).
42. Mangin, S., Montaigne, F. & Schuhl, A. Interface domain wall and exchange bias phenomena in ferrimagnetic/ferrimagnetic bilayers. *Phys. Rev. B* **68,** 140404 (2003).

Author Contributions

K.C., D.L. and F.R. conceived and designed the experiments. K.C. prepared the samples, K.C., F.C., E.O. and P.O. carried out XAS measurements. K.C. and D.L. co-wrote the paper. All the authors discussed the results and commented on the manuscript.

Additional Information

Supplementary information accompanies this paper at http://www.nature.com/srep

Competing financial interests: The authors declare no competing financial interests.

How to cite this article: Chen, K. *et al.* Observation of an atomic exchange bias effect in DyCo$_4$ film. *Sci. Rep.* **5**, 18377; doi: 10.1038/srep18377 (2015).